PROCEEDINGS, 51st Workshop on Geothermal Reservoir Engineering
Stanford University, Stanford, California, February 9-11, 2026
SGP-TR-230

EGS Thermal Recovery Factor from Downhole Engineered Heat Exchangers with Variable Fracture-Driven Interaction Flow Rates

Christine Ehlig-Economides, Nelson Barros-Galvis

Cullen College of Engineering, Department of Petroleum Engineering, University of Houston

ceconomides@uh.edu, nebarros@Central.uh.edu

Keywords: thermal recovery factor, downhole engineered heat exchanger, fracture-driven interaction

ABSTRACT

The injection well profile from the Fervo Energy commercial doublet well configuration shows considerable flow rate variability among multiple hydraulically fractured stages. Even with uniform flow among the fracture-driven interactions (FDIs), recent work suggests that the heal FDI flow rate will be about 16% greater than the rate at the toe of the downhole engineered heat exchanger (DEHE) under the reported circulation rate. This study assesses what fraction of the maximum recoverable heat the DEHE produces as a thermal recovery factor for DEHE configurations of interest.

We define the remaining recoverable heat in a stimulated volume as the energy that can be transferred by reducing its average rock temperature to the final working temperature of the circulating fluid. The model for this study couples models for the flow circulation and heat transfer through the DEHE and the vertical injection and production wells, subject to boundary conditions required for the surface power generation. We define the thermal recovery factor as one minus the time dependent ratio between the original and remaining recoverable heat values, or simply the ratio between the rock temperature change from the original average rock temperature divided by the temperature difference between the original average rock temperature and the lowest plant inlet working fluid temperature for continued plant operation.

Sensitivity studies quantify the variation in thermal recovery factors for a DEHE having identical FDI conductivities with variation between maximum and minimum FDI flow rates from less than 1% to 30%. We then quantify the expected thermal recovery factor for the published Fervo Energy injection well profile.

This study illustrates the importance of the DEHE design and flow conformance on the thermal recovery efficiency of a DEHE. The thermal recovery factor may be improved by a plant workover that enables a lower plant inlet fluid temperature.

1. INTRODUCTION

(Gringarten et al., 1975) offered a vision for an enhanced geothermal system (EGS) that is only recently being realized, first by the Utah FORGE doublet well project using stacked parallel inclined wells that mimic their original diagram. Fervo Energy then used unconventional shale oil and tight gas well construction technology for an analogous approach using laterally parallel horizontal wells for their commercial-scale power generation pilot Project Red (Norbeck et al., 2023) doublet well in Nevada near the FORGE project followed by the Project Cape Station wells in Milford Basin, Utah (Fercho et al., 2024). The Project Red pilot generated a peak of 3.5 MW electric power equivalent, and Project Cape Station includes 18 horizontal wells expected to deliver 75 MW per sq. mi. per bench, with a bench meaning a set of parallel horizontal wells at a given formation depth.

(Asai et al., 2022) emphasized the importance of uniform flow among the fracture driven interactions (FDIs) between the production and injection well in a doublet pattern. (Ehlig-Economides & Barros-Galvis, 2025) noted the importance of FDI conductivity to achieving uniform flow and that, unlike for production wells that require sufficiently high conductivity, sufficiently low conductivity promotes flow uniformity in a doublet pattern.

(Ehlig-Economides & Barros-Galvis, 2026) challenges the current practice of hydraulically fracturing both injection and production wells and suggests that fracturing only injection wells or only production wells will improve FDI flow uniformity and lower well construction costs.

(Zeinali, 2021) and (Stacey, 2025) show that numerical simulation models indicate more pessimistic temperature outlet behavior than that indicated by the analytical model by (Gringarten et al., 1975). The models all assume uniform FDI flow distribution, but the injection rate survey for the Fervo Project Red doublet pattern is not uniform (Norbeck et al., 2023). This paper introduces a new analytical model that more nearly approximates the numerical simulation models. We then use the new analytical model to compare the ideal heat recovery with the model forecast for the Project Red pattern.

2. NEED FOR A NEW ANALYTICAL HEAT TRANSFER MODEL

Figure 1 shows the temperature distribution in the hot dry rock for a numerical simulation model that reproduces the (Gringarten et al., 1975) analytical model applied to the triplet well pattern described in (Ehlig-Economides & Barros-Galvis, 2025) and (Ehlig-Economides & Barros-Galvis, 2026). Figure 2 shows the temperature distribution for the CMG STARS numerical simulation model of the triplet well pattern that includes horizontal injection and production wells (Zeinali et al., 2021). Figure 3 compares the models for several fracture spacing values with solid curves for the analytical model and dashed curves for the numerical simulation model.

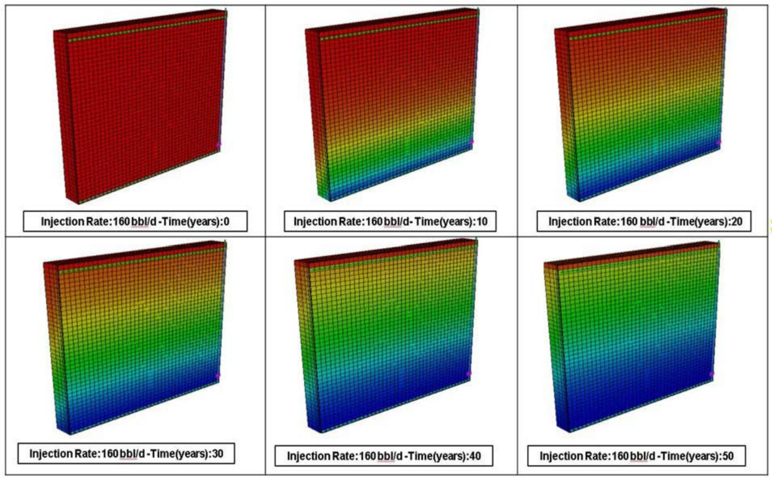

Figure 1:CMG simulations that reproduce (Gringarten et al., 1975) analytical model results (Zeinali, 2021).

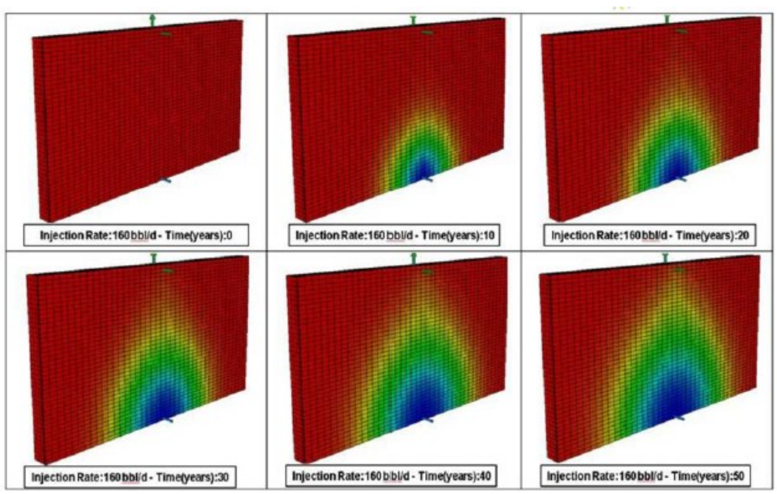

Figure 2: CMG simulations that contrast with (Gringarten et al., 1975) analytical model results (Zeinali, 2021)

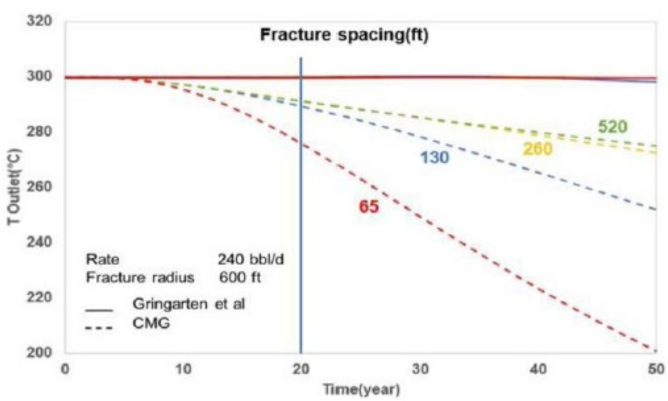

Figure 3: CMG simulated outlet temperatures for several fracture spacing values (Zeinali, 2021).

The comparison in Figure 3 shows that the (Gringarten et al., 1975) analytical model predicts less reduction in produced water temperature over time compared to the numerical simulations. The reason for the discrepancy relates to the well boundary condition geometry used in the analytical model, which treats the well as a line instead of a cylinder intersecting the propped hydraulic fracture through which the circulating fluid flows. The analytical model well geometry results in the linear appearance of the temperature distribution seen in Figure 1 which contrasts distinctly with the radial temperature distribution shown in Figure 2.

The numerical model assumes insulation boundaries corresponding to the vertical and lateral FDI extent because the heat transfer beyond the stimulated formation volume defined by the well length and the series of FDIs is negligible, as is assumed by the analytical model. The models also include an insulation boundary halfway between each pair of adjacent FDIs to represent the temperature interference resulting from identical heat transfer behavior induced by the flow through the adjacent FDIs. Figure 1 shows the temperature distribution away from where the formation face connects to the propped fracture plane. The cooling at the interference boundary lags the cooling of the fluid flowing through the FDI. This same lag effect occurs for the model in Figure 3 and can be seen in a vertical cutaway view through the well location (not shown).

Figure 4 compares the (Gringarten et al., 1975)model with results reported by (Stacey, 2025), which also indicates that the analytical model is overly optimistic.

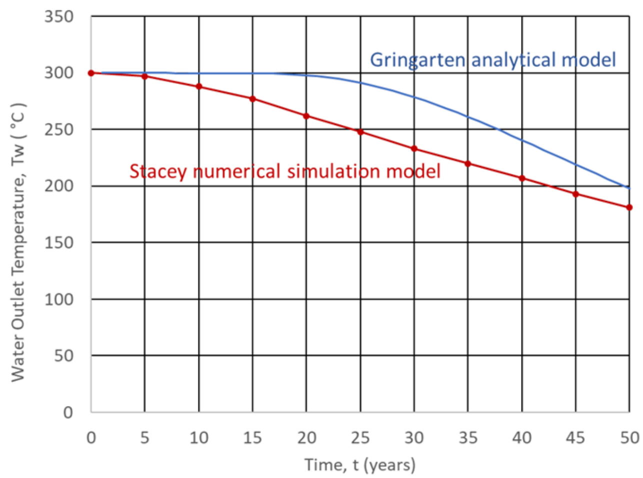

Figure 4: Comparison between modeled outlet temperatures computed by analytical and numerical simulation models

3. HEAT RECOVERY FACTOR

We calculate the thermal recovery factor, R_H, from the outlet temperatures computed from the analytical models using the following equation:

$$R_H = \frac{H_{pw}}{H_{r0}} = \frac{\rho_w c_w q}{2\rho_r c_r A x_E} \int_0^{t_{\text{end}}} \left[1 - \frac{T_{r0} - T_{pw}(t)}{T_{r0} - T_{w0}}\right] dt \tag{1}$$

The conductive heat flow area is $n_f x_f h_f$ whether the horizontal wells are stacked, as for Utah FORGE, or parallel laterals, as for Fervo Energy projects, for the number of fractures, n_f. For the stacked wells each fracture uses half the fracture height, $h_f/2$, and all the fracture length, $2x_f$, while each fracture in a parallel lateral uses all the fracture height and only half the total fracture length. The time, t_{end}, corresponds to when the produced water outlet temperature, $T_{pw}(t_{end}) = T_{plant}$ where T_{plant} represents the lowest bottomhole produced fluid temperature usable by the power plant to generate power at a constant rate. The value of T_{plant} must consider wellbore heat transfer in the production well vertical well segment. Figure 5 compares thermal recovery efficiency for the (Gringarten et al., 1975) and (Stacey, 2025) models for the 40 m spacing case; the blue and red curves in Figure 4 shows the outlet temperatures versus time for the (Gringarten et al., 1975)and (Stacey, 2025) models, respectively.

The two models predict very different thermal recovery factor behavior when computed to an arbitrary time duration. However, assuming that power generation stops when the DEHE outlet temperature drops below the temperature required for power generation, Figure 6 shows that for $T_{r0} - T_{plant} = 5$ °C, the (Stacey, 2025)predicts a lower thermal recovery factor of only about 3% compared to nearly 30% for the overly optimistic (Gringarten et al., 1975)model.

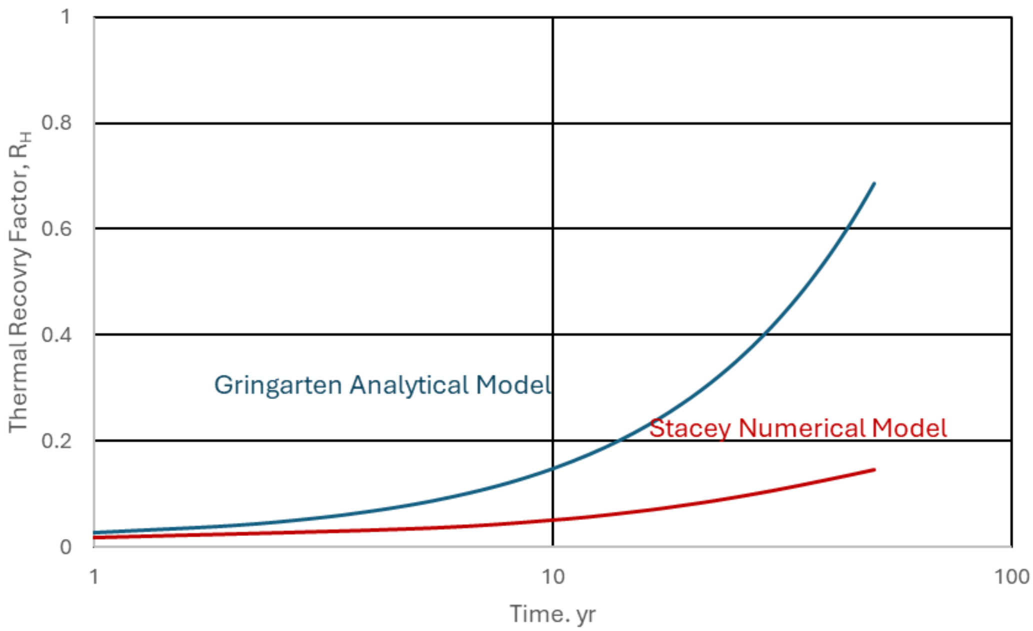

Figure 5: Thermal recovery factor comparison for analytically and numerically modeled outlet temperatures in Figure 4: Comparison between modeled outlet temperatures computed by analytical and numerical simulation models

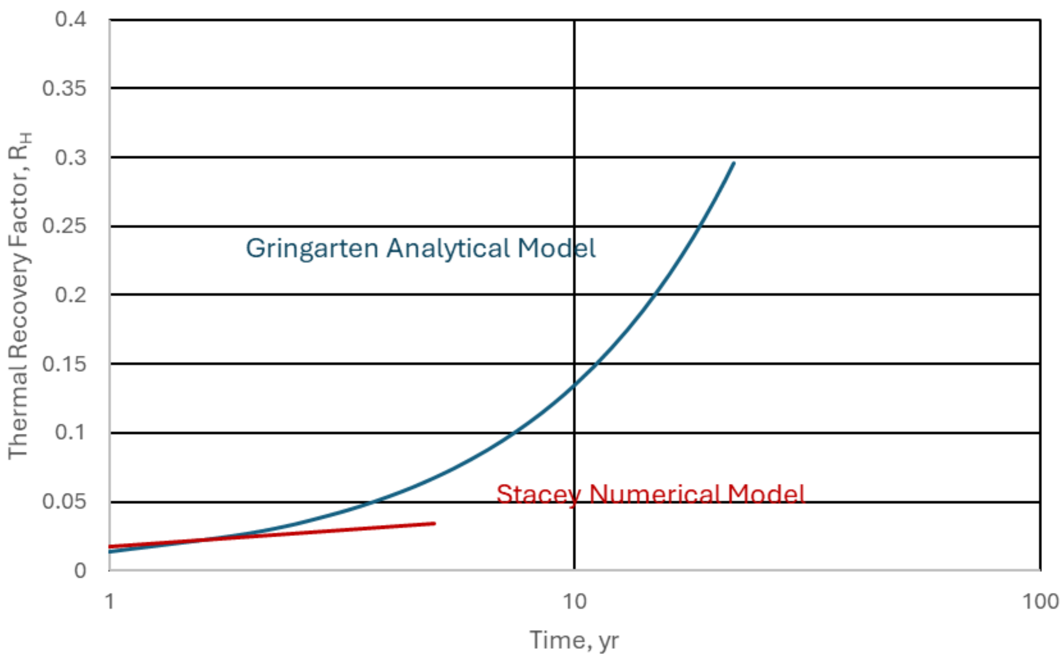

Figure 6: Thermal recovery factor comparison for analytically and numerically modeled outlet temperatures in Figure 4: Comparison between modeled outlet temperatures computed by analytical and numerical simulation models showing only the portion with outlet temperature greater than T_{plant}.

4. FERVO ENERGY PROJECT RED CASE

Results from the Fervo Energy Project Red pilot are encouraging with peak generation at 3.5 MW electric power equivalent (Norbeck et al., 2023). However, the injection flow profile shown in Figure 7 shows rates per stage ranging from zero to 2500 bpd.

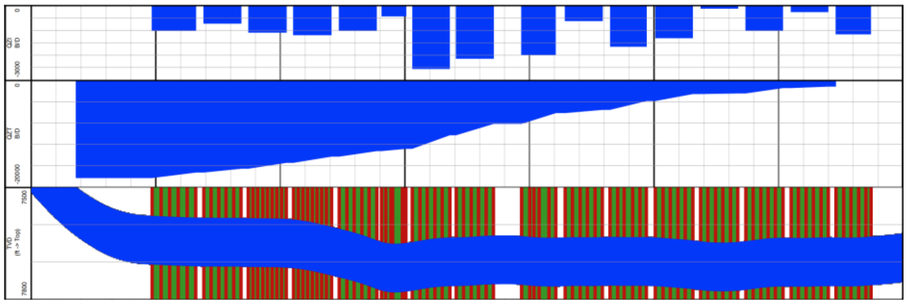

Figure 7: Injection flow profile spinner log survey recorded in Injection Well 34A-22 at a flow rate of 12.5 bpm (Norbeck et al., 2023)

Our analytical model simulations used the data reported by (Norbeck et al., 2023) shown in Table 1. Some of the included data pertain to fluid flow simulations that use a different analytical model (Ehlig-Economides & Barros-Galvis, 2025) that we have not yet coupled with the heat transfer model in this study.

Table 1: Input data for Fervo Energy Project Red analytical model

T_{in}, deg. F	150.8	66 C
T_{wp}, deg. F	336.2	169 C
EHE Depth	7700	2.3 km
Well length, ft	3250	991 m
Injection well diameter, in	7	0.178 m
Production well diameter, in	7	0.178 m
Well roughness,ft	0.00015	
# Hydraulic fractures	96	
Circulation rate, bpd	34209	63.09 kg/s
Injection well bhp, psi	4500	31.03 Mpa
FDI conductivity, md-ft	85	
Hydraulic fracture half-length, ft	365	111 m
Hydraulic fracture height, ft	365	111 m

Summing the rates in Figure 7Figure 7 leads to a total rate of 18997 bpd, but the recorded peak rate was 34209 bpd shown in Table 1. Figure 8 shows the doublet configuration performance that would result for the peak rate with uniform flow among the 96 fractures as the green curve. By way of comparison, this figure also shows the result for the same configuration produced at 1/3 of the peak rate as the blue curve. The temperature rise in the blue curve is an artifact of the (Gringarten et al., 1975) model for low fracture flow rates.

Also shown on the figure is an estimate for the behavior with the nonuniform rates as the burnt orange curve. We computed this result as the flow-rate-weighted temperature average of all 16 stages for each reported stage flow rate behavior estimated as though all 96 fractures had the flow rate for each of the 6 fractures in a stage.

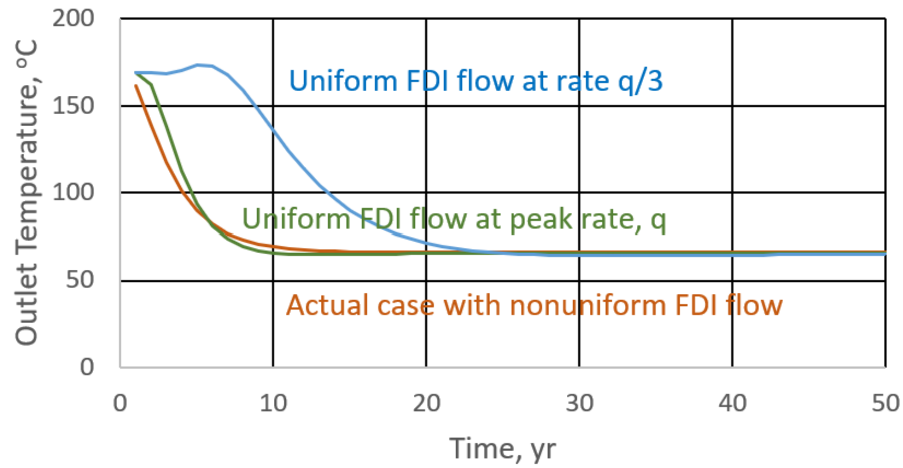

Figure 8: Modeled outlet temperatures for cases related to the Fervo Energy Project Red contrasting the mixed flow rates measured in an injection flow rate survey with uniform FDI flow rates at the reported production rate and one third of that rate.

We note the surprising similarity between the outlet temperature behavior for the same total rate with uniform or nonuniform FDI flow rates, which could suggest that FDI flow uniformity is not critical to the EGS well design. However, Figure 9 forecasts that the Project Red well will not maintain outlet temperature above the assumed T_{plant} value 5 degrees below the starting temperature. In contrast, for the lower flow rate, the outlet temperature is above the T_{plant} limit for about 8 years and is able to reach nearly 30% thermal recovery, as contrasted by the solid blue curve with the dashed curves representing outlet temperatures too low for the assumed power plant requirement. The lower circulation rate will produce less thermal power but is able to successfully extract heat from the formation.

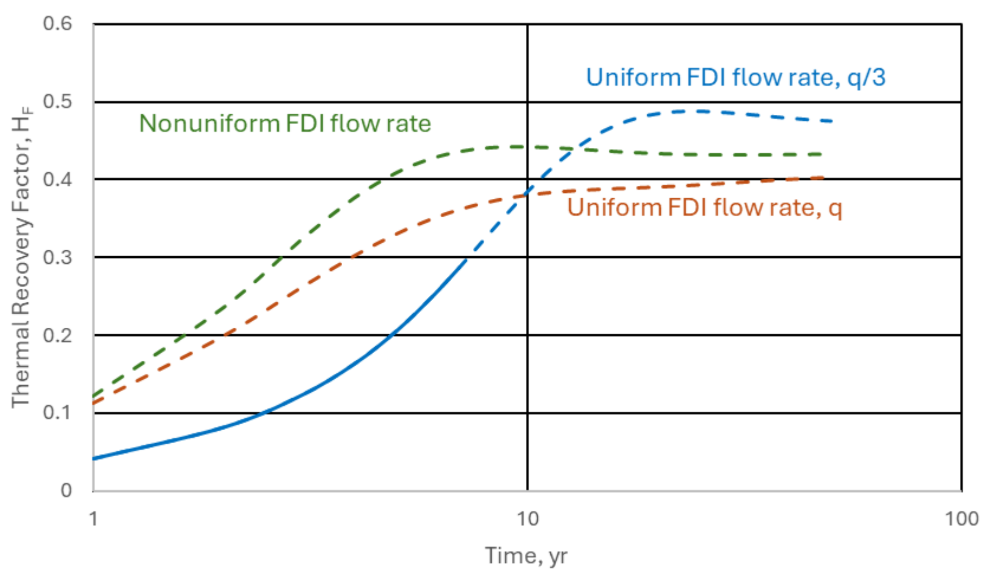

Figure 9: Modeled heat recovery factors for cases related to the Fervo Energy Project Red contrasting the mixed flow rates measured in an injection flow rate survey with uniform FDI flow rates at the reported production rate and one third of that rate.

5. POWER PLANT IMPLICATIONS

When the produced fluid temperature drops, the electric power generation drops. A way to compensate for this is to increase the organic fluid circulation rate through the surface binary fluid exchanger. However, the organic fluid circulation rate must be sufficient to increase the power plant output enough to compensate for the increased energy supplied to the circulation pumps in order to increase the circulation rate. This is why forecasting the produced fluid temperature matters.

Accurate forecasting of the power plant output requires an integrated model coupling power plant performance with vertical well heat transfer models, and the DEHE pressure and heat transfer models.

6. DISCUSSION

Our implementation of the (Gringarten et al., 1975) analytical model produces instabilities like the temperature overshoot seen in the blue curve in Figure 8. We are investigating whether this may be a limitation of the (Stehfest, 1969) algorithm we use for the numerical Laplace Transform inversion.

More importantly, up to now this application of the Gringarten model leads to an unexpected observation that significant variations in FDI flow rates seem to produce greater thermal recovery than uniform flow.

7. CONCLUSIONS

Our analysis suggests that the uniformity of FDI flow had only a relatively small impact on the outlet water temperature, indicating that it may not be a critical factor in EGS design. More importantly, the circulation rate governs thermal sustainability: high circulation rates could potentially cause the outlet fluid temperature to fall below the minimum threshold required for plant operation, while lower rates, although generating less instantaneous thermal power, allow heat extraction over a longer period and achieve nearly 30% thermal recovery. This clearly illustrates the trade-off between maximizing peak output and ensuring sustainable performance.

Similarly, increasing the organic fluid circulation rate does not automatically translate into higher net power output unless the additional power generated by enhanced heat transfer exceeds the corresponding increase in pumping power. For this reason, accurately forecasting the produced fluid temperature is essential, and a prerequisite for realistic power output estimation. Such forecasts require an integrated modeling approach that captures not only power plant performance, but also wellbore heat transfer and the hydraulic and thermal behavior of the DEHE system.

When comparing existing analytical and numerical models, the differences in predicted thermal recovery can be striking. For a realistic operational assumption, namely, that power generation stops when the DEHE outlet temperature falls below the minimum required for electricity production using the following condition: $T_{r0} - T_{plant} = 5$ °C, the numerical model predicted a thermal recovery factor of only about 3%, while the more optimistic analytical model predicted nearly 30%. This clearly shows the importance of accounting for operational limits when assessing both plant performance and reservoir heat extraction.

These findings highlight the need for a new analytical heat transfer model for EGS. Ideally, this model, coupled with models for flow and heat transfer through vertical and horizontal well segments and FDIs should allow for rapid, accurate, and practical evaluation of hot dry rock formation heat transfer behavior and power generation potential, serving as a reliable tool to support project development, EGS design, and operational planning.

ACKNOWLEDGEMENT

The authors wish to thank Utah FORGE for funding this research.

REFERENCES

Asai, P., Podgorney, R., McLennan, J., Deo, M., & Moore, J. (2022). Analytical model for fluid flow distribution in an Enhanced Geothermal Systems (EGS). *Renewable Energy*, *193*, 821–831. https://doi.org/10.1016/j.renene.2022.05.079

Ehlig-Economides, C. A., & Barros-Galvis, N. (2026). A New Approach to Hydraulic Fracturing in Enhanced Geothermal System Well Patterns. *SPE Hydraulic Fracturing Conference*.

Ehlig-Economides, C. A., & Barros-Galvis, N. E. (2025). Role of NonDarcy Flow in Maintaining Uniform Flow among Parallel Propped Hydraulic Fractures in an Engineered Heat Exchanger. *GRC Transactions. Vol. 49*, *49*, 2025.

Fercho, S., Matson, G., Mcconville, E., Rhodes, G., Jordan, R., & Norbeck, J. (2024). Geology , Temperature , Geophysics , Stress Orientations , and Natural Fracturing in the Milford Valley , UT Informed by the Drilling Results of the First Horizontal Wells at the Cape Modern Geothermal Project. 1–12. *PROCEEDINGS 49th Workshop on Geothermal Reservoir Engineering*.

Gringarten, A. C., Witherspoon, P. A., & Ohnishi, Y. (1975). Theory of heat extraction from fractured hot dry rock. *Journal of Geophysical Research*, *80*(8), 1120–1124. https://doi.org/10.1029/jb080i008p01120

Norbeck, J. H., Latimer, T. M., St, M., Norbeck, J. H., & Latimer, T. M. (2023). Commercial-Scale Demonstration of a First-of-a-Kind Enhanced Geothermal System.

Stacey, R. (2025). Enhanced Geothermal Systems (EGS) Modeling with Volsung: Evaluating System Design Geometry and Stimulation Spacing. *GRC Transactions, Vol. 49.*

Stehfest, H. (1969). Algorithm 368 Numerical Inversion of Laplace Transforms. *Communications of the ACM*.

Zeinali, L. (2021). Enhanced Geothermal System Model for Flow Through a Stimulated Rock Volume. 2021 SPE Annual Technical Conference and Exhibition